

# Targeting Exosomal EBV-LMP1 Transfer and miR-203 Expression via the NF- $\kappa$ B Pathway: The Therapeutic Role of Aspirin in NPC

Lielian Zuo,<sup>1,2,5</sup> Yan Xie,<sup>1,2</sup> Jinyong Tang,<sup>3</sup> Shuyu Xin,<sup>1,2</sup> Lingzhi Liu,<sup>1,2</sup> Siwei Zhang,<sup>1,2</sup> Qijia Yan,<sup>1</sup> Fanxiu Zhu,<sup>1,2,4</sup> and Jianhong Lu<sup>1,2</sup>

<sup>1</sup>NHC Key Laboratory of Carcinogenesis, Department of Pathology, Xiangya Hospital, Central South University, Changsha 410080, Hunan, China; <sup>2</sup>The Key Laboratory of Carcinogenesis and Cancer Invasion of the Chinese Ministry of Education, Department of Microbiology, School of Basic Medical Science, Central South University, Changsha 410078, Hunan, China; <sup>3</sup>Department of Otolaryngology-Head and Neck Surgery, the First People's Hospital of Chenzhou, Chenzhou 423000, Hunan, China; <sup>4</sup>Department of Biological Science, Florida State University, Tallahassee, FL 32306, USA; <sup>5</sup>Institute of Neuroscience, Medical College, University of South China, Hengyang 421001, Hunan, China

**Nasopharyngeal carcinoma (NPC) is an invasive head-and-neck tumor with Epstein-Barr virus (EBV) as an important etiological cause. The EBV oncoprotein Latent membrane protein 1 (LMP1) can be trafficked into exosomes with unclear roles, and this trafficking is a potential problem in NPC control. MicroRNA-203 (miR-203) was found by us to be downregulated by LMP1, and it functions as a tumor suppressor in NPC. In this study, aspirin reversed the epithelial-mesenchymal transition (EMT) by promoting miR-203 expression in cells, and, remarkably, it repressed exosomal LMP1 (exo-LMP1) secretion from EBV-positive cells. Nuclear factor  $\kappa$ B (NF- $\kappa$ B) activation was required for the exo-LMP1 production. The exo-LMP1 uptake influenced the EMT potential of EBV-negative recipient NPC cells. The exo-LMP1 level was upregulated in clinical NPC plasma samples. Aspirin treatment observably inhibited NPC lung metastasis in nude mice. The study revealed that aspirin is a promising drug for NPC therapy via its targeting of exo-LMP1 transfer and the regulatory effect of LMP1 on miR-203 expression. EBV can regulate its own tumorigenesis via the LMP1/NF- $\kappa$ B/exo-LMP1 axis, opening a new avenue for understanding the pathogenesis of this tumor virus. Our study also provides a rationale for the use of exo-LMP1 or exosomal miR-203 (exo-miR203) in EBV-targeted therapy by aspirin in invasive NPC.**

## INTRODUCTION

Epstein-Barr virus (EBV) is a major human pathogen that is tightly linked to the development of several malignancies, including nasopharyngeal carcinoma (NPC), which is prevalent in southern China.<sup>1-3</sup> NPC is an aggressive head-and-neck tumor of epithelial origin.<sup>4-6</sup> Although a combination of chemotherapy and radiotherapy is the current therapeutic approach, metastatic relapse is still an important failure point in NPC treatment. Due to its special pathogenic site and lack of specific early symptoms, NPC is always first diagnosed at a late stage. The resistance of NPC to

chemotherapy and radiotherapy is the next vexing problem. Therefore, suitable drugs and novel biomarkers are worthy of exploration to improve the prevention, detection, and therapy of NPC. Undoubtedly, there are broad prospects for the development of EBV-targeted treatment and diagnosis in this kind of virus-associated cancer.

Latent membrane protein 1 (LMP1) is the confirmed EBV oncoprotein. LMP1 has transforming properties *in vitro* and is frequently expressed in EBV-associated cancers.<sup>7-9</sup> LMP1 constitutively activates the nuclear factor  $\kappa$ B (NF- $\kappa$ B)-signaling pathway in NPC.<sup>10-12</sup> In our previous study, we showed that LMP1-activated NF- $\kappa$ B inhibited the expression of microRNA-203 (miR-203), which functions as a switch to maintain the normal phenotype of nasopharynx epithelial cells.<sup>10,13</sup> As this switch is hijacked and cut off by EBV-encoded LMP1 (EBV-LMP1), miR-203 expression is downregulated. Our experimental evidence highlighted miR-203 as an active player in the inhibition of several key steps in tumorigenesis, including tumor growth, the epithelial-mesenchymal transition (EMT), invasion, and metastasis of NPC.<sup>10,13</sup> The EMT is an important early step in cancer metastasis.<sup>2,13</sup> As is already known, microRNAs (miRNAs) play critical regulatory roles in cellular biology and cancer development by inhibiting the transcription and translation of their targets.<sup>2,10,13</sup> In related studies, cadherin 6 (CDH6), RUNX2, and E2F3 have been identified as direct targets of miR-203.<sup>10,13,14</sup> Furthermore, other groups have revealed that low miR-203 expression in NPC tissue was related to tumor stemness and the resistance of the cancer to chemotherapy and radiotherapy,<sup>15,16</sup> miR-203 downregulation is related to poor prognosis in NPC patients.<sup>13,15,16</sup> Therefore, we

Received 11 April 2019; accepted 22 May 2019;  
<https://doi.org/10.1016/j.omtn.2019.05.023>.

**Correspondence:** Jianhong Lu, NHC Key Laboratory of Carcinogenesis, Department of Pathology, Xiangya Hospital, Central South University, Changsha 410080, Hunan, China.

**E-mail:** [jianhlu@csu.edu.cn](mailto:jianhlu@csu.edu.cn)



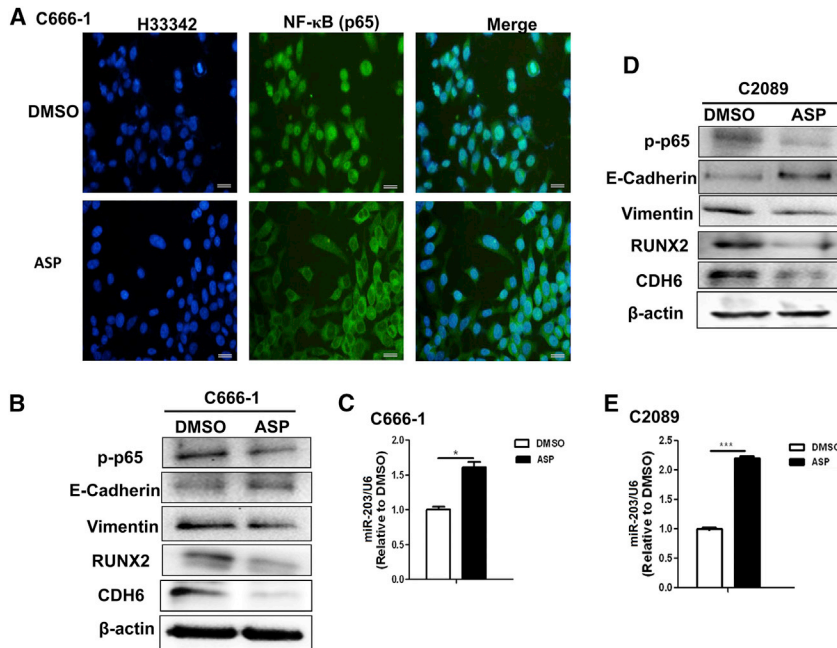


**Figure 1. Aspirin Treatment Inhibits the EMT and Promotes miR-203 Expression in EBV-Positive Cells**

(A) Representative images showing that aspirin (ASP) treatment inhibited the activation and nuclear entry of NF-κB (p65). An IF assay was used for p65 detection. Scale bars, 50 μm. (B) The detection of the EMT markers phosphorylated p65 (p-p65), RUNX2, and CDH6 in NPC C666-1 cells by WB at 36 h after ASP treatment. E-cadherin is an epithelial marker and vimentin is a mesenchymal marker. (C) The detection of miR-203 expression level in C666-1 cells by qPCR. (D) The detection of the EMT markers p-p65, RUNX2, and CDH6 in C2089 cells by WB following ASP treatment. (E) The detection of miR-203 in C2089 cells by qPCR. The results are the means ± SD from three independent experiments (n = 3). \*p < 0.05, \*\*p < 0.01, \*\*\*p < 0.001.

were interested in how this miR-203-controlled perfect switch could be used for NPC therapy and diagnosis.

Extracellular vesicles (EVs) are released by most cell types, including tumor cells and other cells within the tumor microenvironment. Exosomes are the main subpopulation of EVs, with sizes ranging from 30 to 150 nm.<sup>17,18</sup> Exosomes have been validated as important mediators of cell-cell communication by transferring bio-macromolecules, including oncoproteins, DNA, miRNA, mRNA, and other bioactive molecules.<sup>17,18</sup> Emerging evidence has demonstrated that exosomes released from tumor cells may affect tumor formation, growth, metastasis, and drug resistance. Furthermore, circulating exosomal cargo may be useful as reliable cancer biomarkers.<sup>19–22</sup> LMP1 was previously reported to be secreted from EBV-positive tumor cells via exosomes.<sup>23</sup> However, we have only a minimal understanding of the bioactivity of exosomal viral proteins. Recently, exosomal PD-L1 was revealed as an important factor in the failure of cancer immunotherapy.<sup>24,25</sup> This finding is a reminder of the need to examine the functions of exosomal LMP1 (exo-LMP1), and, especially, of the importance of exploring novel drugs to restrict exosome-mediated LMP1 transfer.

As mentioned above, EBV-LMP1-activated NF-κB induces the growth, EMT, and metastasis of NPC by inhibiting the host switch, miR-203.<sup>13</sup> We have confirmed that this effect was reversible by using a chemical inhibitor of NF-κB. Aspirin is a non-steroidal anti-inflammatory drug (NSAID) and can act as an NF-κB inhibitor, and it has already been used in colorectal cancer therapy.<sup>26,27</sup> Substantial evidence from studies of other cancers indicates that aspirin is an attractive potential anti-tumor agent, and it has been proposed that it might be useful for the prevention of colorectal cancer.<sup>27</sup> In the present study,

we attempted to use aspirin to reverse the function of the LMP1/miR-203 axis in EBV-associated NPC. Because circulating proteins and miRNAs are easily applied clinically, we assessed the exo-LMP1 and miR-203 expression levels in clinical NPC specimens and aspirin-treated cells. Interestingly, we found that the exo-LMP1 secretion from cells was dramatically suppressed by aspirin treatment. At the same time, the miR-203 expression levels in the cells and exosomes were increased. The clinical samples exhibited high exo-LMP1 and low miR-203 levels, suggesting a potential therapeutic use for aspirin in clinical settings. Aspirin also significantly restricted NPC metastasis in an animal model. The results revealed aspirin as a promising tool for NPC therapy.

## RESULTS

### Aspirin Reverses the EMT Induced via the Functional NF-κB/miR-203/CDH6 Axis

Our previous study revealed that LMP1-activated NF-κB inhibits miR-203 expression, which can block the EMT by targeting both CDH6 and RUNX2 in EBV-associated NPC.<sup>10,13</sup> RUNX2 is also a CDH6 activator.<sup>28,29</sup> The results demonstrated that aspirin reversed the functional NF-κB/miR-203/CDH6/EMT axis in EBV-positive cells (Figure 1). The NF-κB, with p65 as its major subunit, can enter the nucleus when activated via phosphorylation. As shown in Figure 1A, aspirin treatment inhibited the activation and nuclear entry of NF-κB (p65) in the EBV-positive C666-1 NPC cells. Further experimentation showed that the miR-203 expression was restored, and both miR-203 target genes (RUNX2 and CDH6) were significantly downregulated in the EBV-positive C666-1 and C2089 cells (Figures 1B–E). Furthermore, the EMT induction was inhibited in both cell lines, as shown by assessing EMT markers (Figures 1B and 1D).

### Aspirin Suppresses the Exosomal Secretion of LMP1 and Promotes miR-203 Expression

Since aspirin had an effect on miR-203 expression and the EMT (Figure 1), we further attempted to assess whether the exosomes could also be influenced by the drug. Consistent with the result shown in

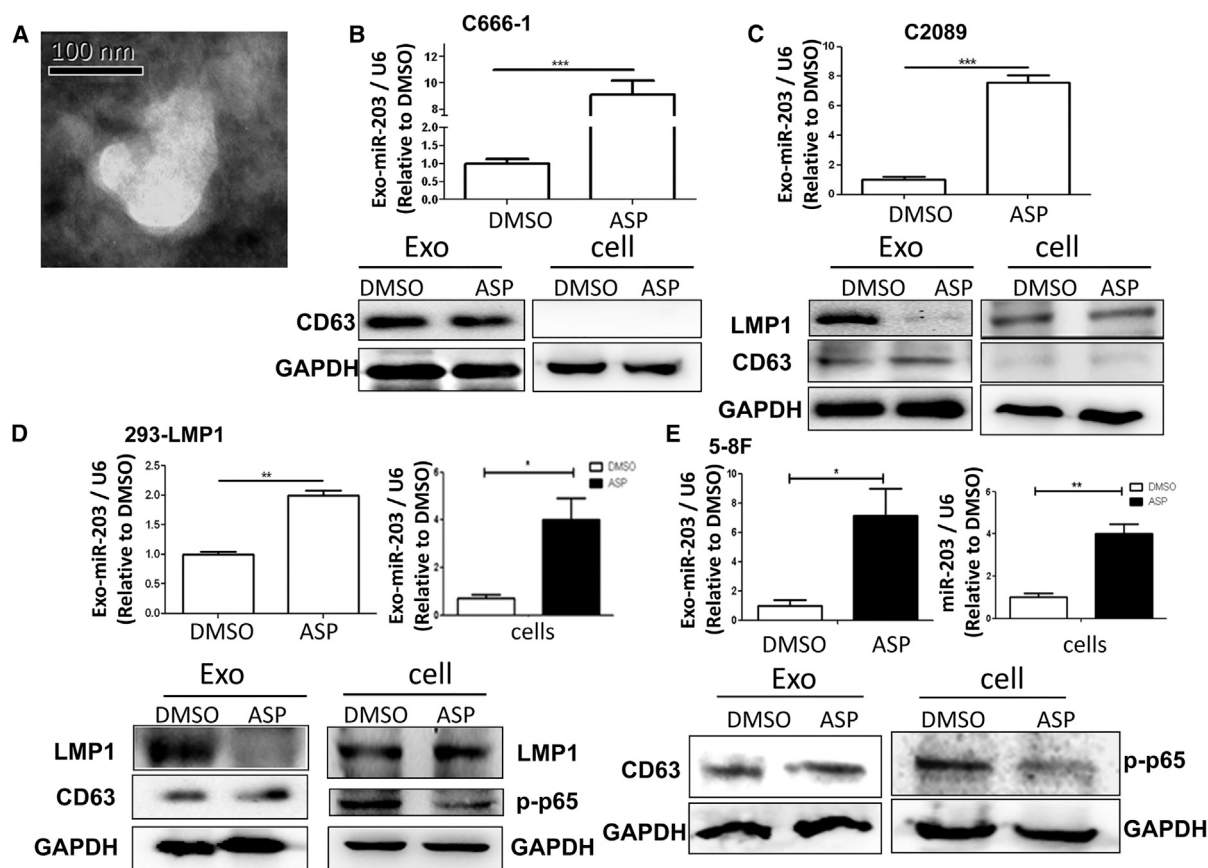


**Figure 2. ASP Efficiently Represses Exosomal LMP1 (exo-LMP1) Secretion and miR-203 Expression in Cells**

(A) A representative TEM image of the exosomes from C666-1 cells. (B) The detection of exosomal miR-203 and CD63 (a marker of exosomes) in C666-1 cells. C666-1 is an NPC cell line expressing very low levels of LMP1. Exo, exosomes. (C) The detection of LMP1, miR-203, and CD63 in C2089 cells and their exosomes. (D) The detection of LMP1, miR-203, CD63, and p-p65 in 293-LMP1 cells and their exosomes. (E) The detection of miR-203, CD63, and p-p65 in 5-8F cells and their exosomes. The results are the means  $\pm$  SD ( $n = 3$ ). The tested samples were collected 24 h post-treatment. \* $p < 0.05$ , \*\* $p < 0.01$ , \*\*\* $p < 0.001$ .

Figure 1 (for C666-1 and C2089 cells), miR-203 expression was also improved in 293-LMP1 and 5-8F cells at different levels following aspirin treatment (Figures 2D and 2E). Consistent with the miR-203 expression in the cells, the exosomal miR-203 levels from all of the cell lines were also elevated following aspirin (ASP) treatment. For the C666-1 and C2089 cells, the exosomal miR-203 levels were remarkably improved ( $p < 0.001$ ) (Figures 2B and 2C), suggesting the enrichment of exosomal miR-203 by aspirin treatment. Aspirin did not obviously affect LMP1 expression in cells 24 h post-treatment, but it dramatically inhibited the exosomal secretion of LMP1 from LMP1-positive cells (Figures 2C and 2D).

#### NF- $\kappa$ B Activation Is Required for the Regulation of LMP1 Trafficking into Exosomes

As connections between both LMP1 and miR-203 and the NF- $\kappa$ B-signaling pathway have been unveiled, we attempted to determine whether NF- $\kappa$ B inhibition is linked to exo-LMP1 secretion and miR-203 expression. First, rescue of NF- $\kappa$ B (p65) by p65 transfection in aspirin-treated C2089 cells restored the level of exo-LMP1 (Fig-

ure 3A). Second, 293-LMP1 cells were treated with a specific NF- $\kappa$ B chemical inhibitor and transfected with p65. The results showed that the exo-LMP1 level was suppressed by the inhibitor and upregulated by p65 overexpression (Figure 3B). These results validated the prediction that NF- $\kappa$ B inhibition contributed to the modulatory role of aspirin on LMP1 trafficking into exosomes.

#### exo-LMP1 Uptake Induces the EMT Potential in EBV-Negative NPC Cells

It is known that no more than 70% of the tumor cells are LMP1 positive in EBV-related NPC tissues.<sup>30</sup> As the viral oncoprotein LMP1 is important in the cancer progression, immune subversion, and therapy resistance of EBV-related NPC,<sup>7-12</sup> we speculated that exo-LMP1 may also have a potential role when taken up intracellularly by EBV-negative NPC cells. To detect the bioactivity of exo-LMP1, exosomes from 293-LMP1 cells and control (293-vector) cells were co-cultured with EBV-negative 5-8F and HK-1 cells. As shown in Figure 4, the uptake of exo-LMP1 resulted in miR-203 downregulation and EMT promotion in the recipient cells. In these experiments,

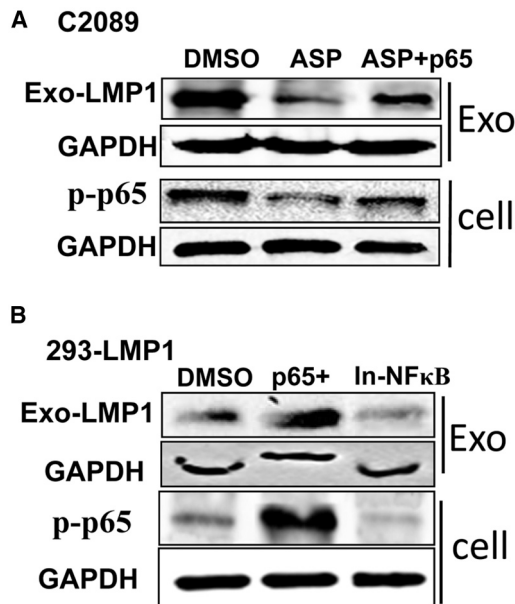


**Figure 3. Rescue of exo-LMP1 by Elevated NF-κB Activation**

(A) The exo-LMP1 expression 24 h after ASP treatment and NF-κB (p65) recovery in C2089 cells. ASP + p65, p65 was overexpressed and ASP was present in the medium simultaneously. (B) The exo-LMP1 expression 24 h after p65 overexpression (p65+) or NF-κB inhibitor (In-NF-κB) treatment in 293-LMP1 cells.

the miR-203 target CDH6 was used as a mesenchymal marker in the NPC cells. We also assessed the role of exosomal miR-203 in EBV-positive C666-1 cells and highly metastatic 5-8F cells. The results demonstrated that the uptake of exosomal miR-203 inhibited the EMT potential of C666-1 and 5-8F cells (Figure S1). These results showed that both exo-LMP1 and exosomal miR-203 had similar bioactivities in cells to those of their cellular forms.

#### exo-LMP1 Is Upregulated and Exosomal miR-203 Is Downregulated in NPC Plasma

As we know that LMP1 is upregulated and miR-203 is downregulated in NPC tissue, here we attempted to measure the exo-LMP1 and miR-203 levels in NPC plasma. The results showed that the differences in their levels are consistent with those observed in tumor tissue (Figure 5C). In particular, NPC-derived exo-LMP1 is dramatically upregulated relative to the normal controls ( $p < 0.001$ ), with more than 75% of those from NPC above the normal mean level. The exosomal miR-203 (exo-miR203) levels of more than 85% of the samples were above the normal mean level. Furthermore, we analyzed the relative levels of exo-LMP1 and exosomal miR-203 in clinical samples from the same patient and from a normal person (Figures 5D and 5E). Overall, the exo-LMP1 levels were high and the exo-miR203 levels were low for the same patient. In a subset of the samples (for example, T39–T47), the exo-LMP1 level was relatively low and the miR-203 level was relatively high. These results confirmed that the relative amounts of LMP1 and miR-203 packaged into exosomes were inversely related.

#### Aspirin Treatment Inhibits NPC Cell Metastasis in Nude Mice

The 5-8F NPC cell line is highly metastatic. To observe the effect of aspirin on NPC metastasis, the drug was added daily into the drinking water of nude mice after venous inoculation of 5-8F cells. During the experimental process, we found that the mice in the drug treatment group were much more active, while those in the control group exhibited dispirited behavior, inappetence, and dyspnea soon after the cancer cell inoculation. At the end of the experiment, the mean body weight of the mice in the drug group was significantly higher than that of the control group (Figure 6A).

There were surprisingly fewer and smaller metastatic tumor nodes in the lungs of the aspirin-treated mice (Figure 6B). No metastatic nodes were found in other organs and tissues. There was no difference in the liver weights between the mice in both groups (Figure 6C). The appearance of the lungs and the H&E staining of lung sections also showed significant differences between the treated and untreated mice (Figures 6D and 6E). As CDH6 expression is relatively high in 5-8F cells<sup>13</sup> and undetectable in lung tissues, we monitored CDH6 to track the metastatic tumor cells. The results showed that NPC cancer cells filled in the alveolar spaces in some fields of view of the samples from the control group (Figure 6F), whereas most areas of the lungs looked normal in the drug treatment group (Figure 6F).

#### DISCUSSION

EVs, especially exosomes, allow tumor cells to deliver certain types of information to recipient cells. Tumor-derived exosomes are like drones that can move outside the original cells to regulate tumor microenvironments, to facilitate tumor growth and metastasis, or even to battle the host immune system, which can limit the response to immunotherapy.<sup>18,19,24,31,32</sup> A growing body of evidence has demonstrated that exosomes contain functional products of viruses, particularly viral oncoproteins such as EBV-encoded LMP1.<sup>18,33,34</sup> It is consequential to explore novel drugs to restrict exosome-mediated LMP1 transfer.

Differential miRNAs have been identified in NPC and are available in databases,<sup>35</sup> implying their potential roles in NPC development. We have known that NF-κB inhibits the expression of miR-203, and our previous study revealed that miR-203 is an LMP1/NF-κB target and it acts as a switch, with multiple roles in sustaining the normal phenotype of nasopharynx cells.<sup>10,13</sup> As aspirin can act as an NF-κB inhibitor,<sup>26</sup> we attempted applying the drug's effect on the EMT of EBV-positive cells. Although the results were as expected, they confirmed, for the first time, the anti-invasiveness property of aspirin in EBV-associated NPC. The restoration of miR-203 expression in the tumor cells following aspirin treatment supported the possibility that aspirin could be effectively used for NPC therapy. These results suggest a prospective novel use for aspirin, which is inexpensive and beyond therapeutic resistance.

Here we showed that the activation or inhibition of NF-κB promoted or suppressed LMP1 packaging into exosomes, respectively. The results showed that exo-LMP1 was rapidly inhibited by aspirin within 24 h post-treatment (Figure 2). However, LMP1 expression in cells



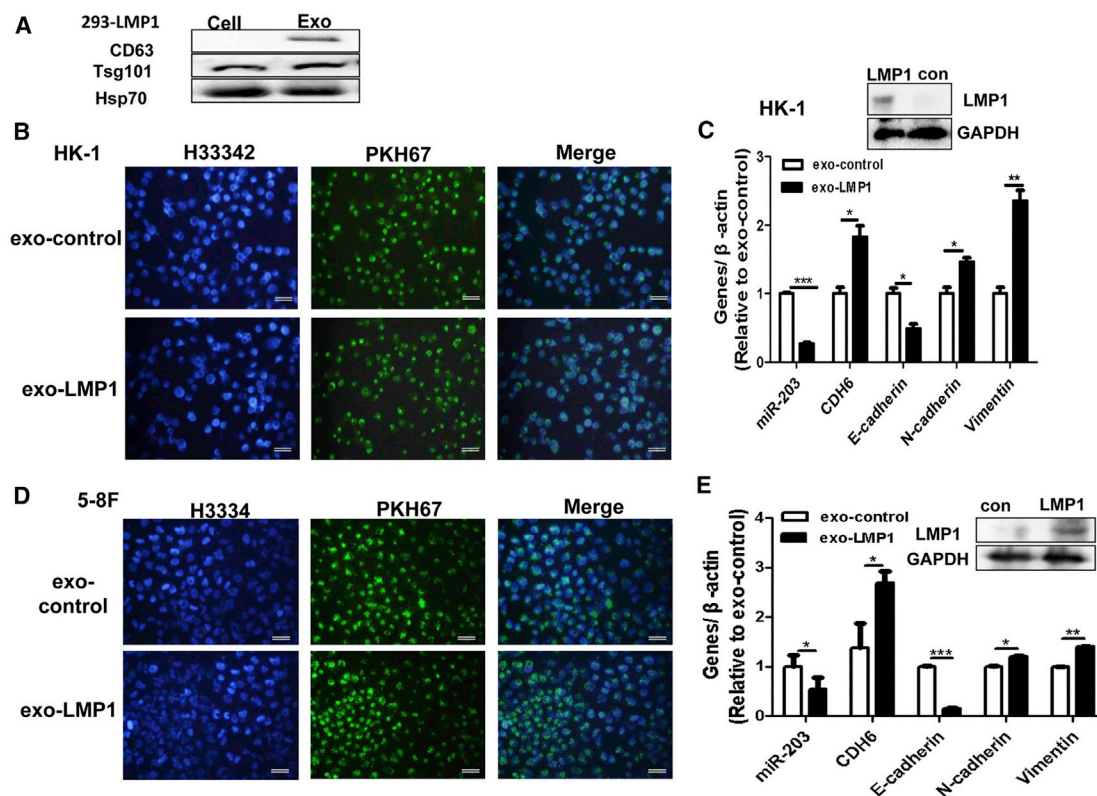


**Figure 4. exo-LMP1 Uptake Induces EMT Potential in Recipient EBV-Negative NPC Cells**

(A) The detection of exosome markers by WB. The exosomes (Exo) were derived from 293-LMP1 cells. (B) HK-1 NPC cells co-cultured with exo-LMP1. Exo-control (con) exosomes were derived from a control 293 cell line stably transfected with a vector.<sup>13</sup> (C) The detection of LMP1, miR-203, CDH6, and the EMT markers in HK-1 cells after co-culture. N-cadherin and vimentin are mesenchymal markers. (D) HK-1 NPC cells co-cultured with exo-LMP1. In (B) and (D), green indicates PKH67-labeled exosomes and blue indicates cell nuclei with H33342 staining. Scale bar, 50  $\mu$ m. (E) The detection of LMP1, miR-203, CDH6, and the EMT markers in 5-8F cells after co-culture. The results are the means  $\pm$  SD (n = 3). \*p < 0.05, \*\*p < 0.01, \*\*\*p < 0.001.

seemed to be not impacted so rapidly. As it is known, the expression of viral LMP1 is largely dependent on the replication of the EBV genome, which is carried out with the host cell cycle.<sup>36</sup> This is a relatively slow process. Because LMP1 is known to constitutively activate NF- $\kappa$ B in cancer, here LMP1 is implicated in the regulation of its own trafficking into exosomes via the NF- $\kappa$ B pathway. On the other hand, targeting LMP1-activated NF- $\kappa$ B by aspirin repressed the delivery of exo-LMP1. These results further implied that aspirin could be an effective solution both for fighting cancer cells and for targeting cell-derived exo-LMP1 in EBV-associated NPC.<sup>1,37</sup> It has been reported that CD63 also regulates exo-LMP1 release, thus impacting the LMP1-dependent induction of the NF- $\kappa$ B pathway.<sup>38,39</sup> As CD63 is a known exosomal marker, it is reasonable to expect that it is required for exosome packaging. We thus speculate that the exo-LMP1 secretion can be somewhat a result of the interaction between the CD63 and NF- $\kappa$ B pathway.

Whether exo-LMP1 has bioactivity remains to be well understood. Our results indicated that EBV-positive cells may influence EBV-negative cells by transferring exo-LMP1. The exo-LMP1 promoted

and miR-203 inhibited the EMT potential of recipient NPC cells, probably due to the opposite effects of NF- $\kappa$ B on exo-LMP1 and miR-203 expressions.

In the animal experiment, it was clear that oral aspirin treatment (upon which the aspirin enters the bloodstream) suppressed tumor metastasis. Remarkably, these results further indicated a therapeutic role for aspirin in invasive NPC.

The testing of liquid biopsies is non-invasive and very attractive, especially for NPC, as it is a small tumor from which it is inconvenient to obtain samples. The feasibility of exo-LMP1 detection supports that such an approach could be a promising option for NPC diagnosis. However, this observation also raises a concern regarding the control of NPC, since exo-LMP1 can be secreted and reach afar. In light of this challenge, determining the best approach for aspirin application is the next topic of our work.

In summary, we revealed a promising therapeutic role for aspirin in the treatment of invasive NPC via its targeting of exo-LMP1 transfer

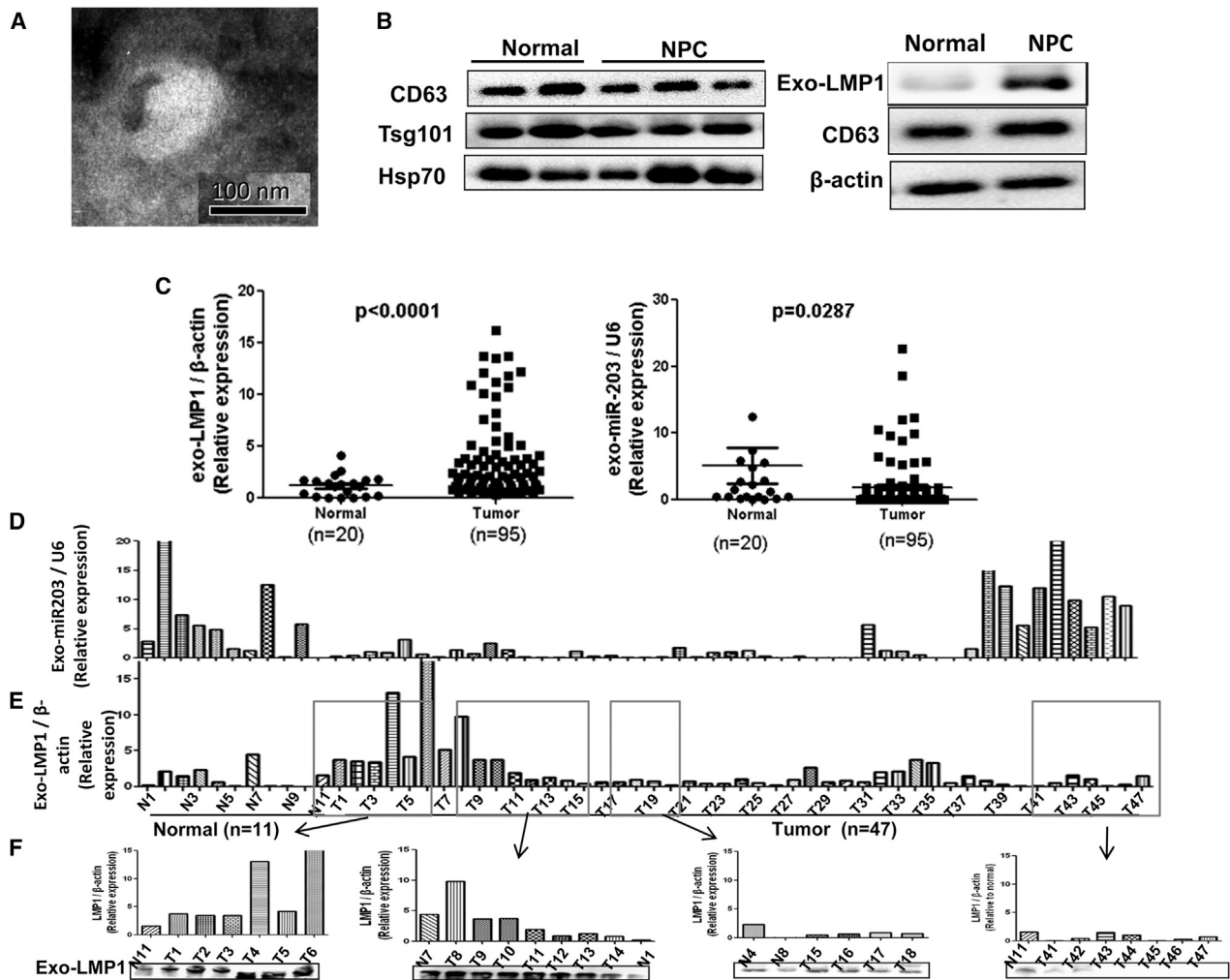


**Figure 5. The Detection of exo-LMP1 and miR-203 in Clinical NPC Plasma**

(A) A representative TEM image of exosomes from NPC plasma. (B) The detection of exosome markers and exo-LMP1 by WB. (C) The analysis of exo-LMP1 and miR-203 levels in clinical NPC plasma samples. (D) Relative values for the exo-miR203 levels from each of the samples (for NPC tumor,  $n = 47$ ). (E) Relative values for the exo-LMP1 levels from each of the samples. The serial number of each sample in (D) and (E) was the same. (F) The samples in the boxes in (E) were used for comparison of the mRNA (qPCR) and protein (WB) levels. The results are the means  $\pm$  SD ( $n = 3$ ). \* $p < 0.05$ , \*\* $p < 0.01$ , \*\*\* $p < 0.001$ .

and modulation of miR-203 expression. Aspirin could inhibit the EMT in both EBV-positive and EBV-negative cells via the functional NF- $\kappa$ B/miR-203/CDH6 axis. The host exosome pathway was hijacked by EBV to modulate intercellular communication. NF- $\kappa$ B activation was required for the regulation of LMP1 trafficking into exosomes. This finding demonstrated that LMP1 can regulate its own transport into exosomes via NF- $\kappa$ B activation and, subsequently, contribute to tumor progression, which is also a newly uncovered function of LMP1. These results opened a new avenue for the understanding of the pathogenesis of this tumor virus. exo-LMP1 was shown to be useful as a biomarker for non-invasive diagnosis of EBV-associated NPC and for evaluating the effects of aspirin treatment. Because miR-203 is a target of the LMP1/NF- $\kappa$ B pathway, the expression levels of cellular and exosomal miR-203 can be influ-

enced by aspirin. Therefore, miR-203 levels could also be a potential biomarker for NPC diagnosis and therapy. Our study provides rationales for the application of exo-LMP1 or exo-miR203 for aspirin-based EBV-targeted or NF- $\kappa$ B-targeted therapy in invasive NPC.

## MATERIALS AND METHODS

### Cell Lines and Plasmids

Human NPC cell lines (5-8F, HK-1, and C666-1) and HEK293 and 293 cells were maintained in our laboratory as previously described.<sup>13</sup> Both the HK-1 and 5-8F cell lines are EBV negative, and 5-8F cells are highly metastatic.<sup>40-43</sup> C666-1 is EBV positive but expresses low-to-undetectable levels of LMP1.<sup>44</sup> We previously established that C2089 harbors the entire EBV genome (p2089).<sup>45-47</sup> The 293-LMP1 and 293-miR203 cell lines were established previously via

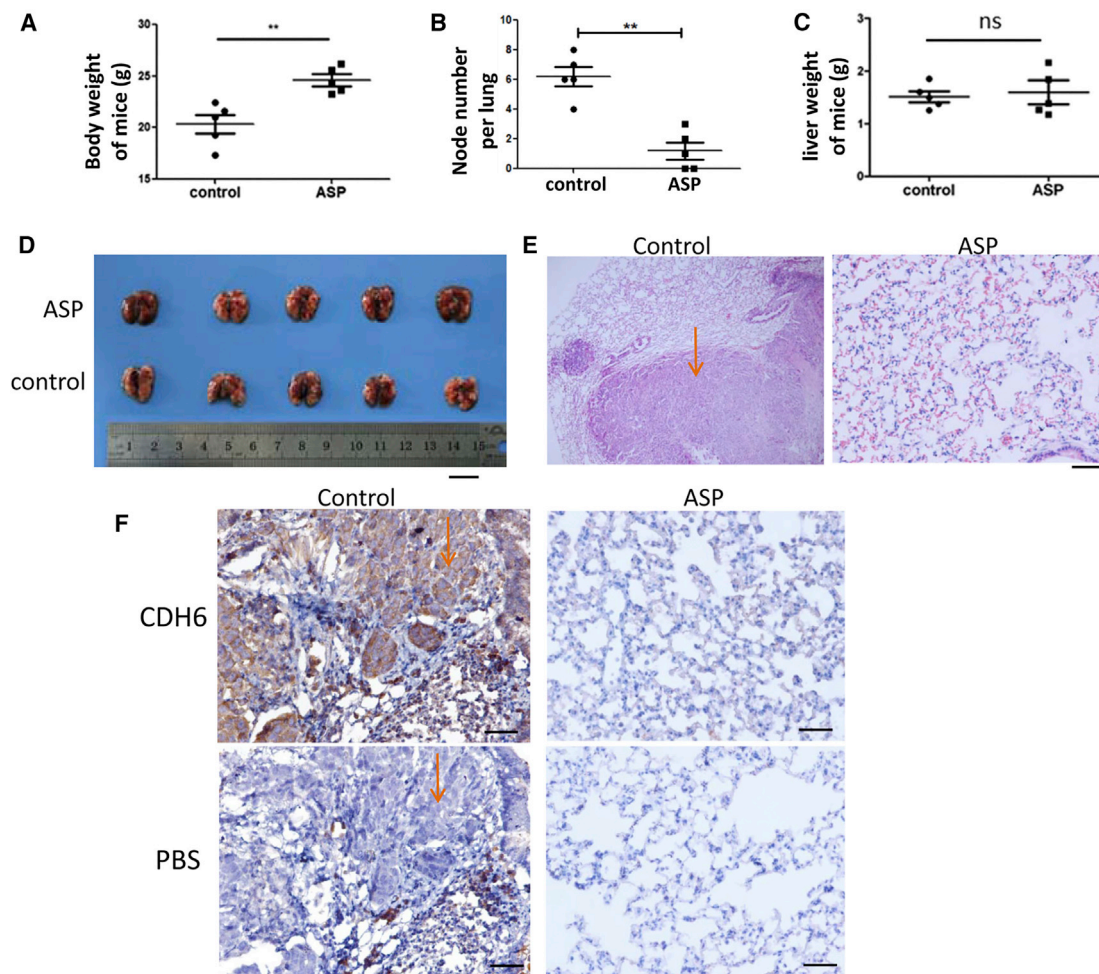


**Figure 6. The Effect of Oral ASP on NPC Metastasis in Nude Mice**

(A) The body weight comparison of the nude mice with and without ASP treatment. Control, ethyl alcohol. \*\* $p < 0.01$ . (B) Comparison of the metastatic node numbers in the lungs from mice in both groups. \*\* $p < 0.01$ . (C) Comparison of the liver weights from mice in both groups. ns, no significance. (D) Appearance of mouse lungs. Scale bar, 10 mm. (E) Histopathological examination of the metastatic tumors in the lungs by H&E staining. The arrow indicates the tumor location in the control. Scale bar, 50  $\mu$ m. (F) Detection of CDH6 by IHC analysis for tracking the 5-8F tumor cells. Serial sections were used. PBS was used as a control corresponding to the CDH6 antibody in the IHC detection. The arrows indicate that tumor cells filled in the pulmonary alveoli. Scale bar, 100  $\mu$ m.

stable transfection of LMP1 and miR-203 expression plasmids, respectively.<sup>13</sup> We previously constructed a p65 (NF- $\kappa$ B) expression plasmid.<sup>13</sup> The cell lines were cultured in RPMI1640 (for the NPC cells) or DMEM (for the 293 and 293-derived cells), supplemented with 10% fetal calf serum (FCS) at 37°C in a humidified atmosphere containing 5% CO<sub>2</sub>.

#### Exosome Extraction from Cells and Plasma

To eliminate interference from fetal bovine serum (FBS)-derived exosomes in the cell culture medium, the FBS was centrifuged at 15,000  $\times g$  for 15 h. When the cells reached 70%–80% confluence in 100-mm dishes, the culture medium was replaced with medium containing 10% exosome-free FBS. After 36 h of incubation, the cell supernatant was collected, and 15 mL supernatant was centrifuged

at 3,000  $\times g$  for 15 min to remove cells and cell debris. The exosomes were extracted from the cells using an ExoQuick-LP kit (System Biosciences, USA) with ExoQuick and Exosome Precipitation Solution (System Biosciences). An appropriate volume of the exosome precipitation reagent was added to the collected supernatant, and the solution was incubated for 12 h on a tube rotator at 4°C. Next, the tube was centrifuged at 1,400 rpm for 10 min. The pellet containing the lipoprotein-depleted exosomes was used for further applications. The purified exosomes were subjected to morphological analysis by transmission electron microscopy (TEM).<sup>48</sup>

#### Exosome Labeling and Co-culture with Cells

The PKH67 Green Fluorescent Cell Linker Kit (Sigma-Aldrich) was used for the exosome labeling. The labeling vehicle (diluent c) provided



in the kit is an aqueous solution designed to maintain cell viability and maximize staining efficiency. Exosomes containing approximately 10–20  $\mu\text{g}$  proteins were first resuspended in 100  $\mu\text{L}$  PBS and subsequently diluted in 250  $\mu\text{L}$  diluent c, while 1  $\mu\text{L}$  fluorescein isothiocyanate (FITC)-PKH67 was diluted in 250  $\mu\text{L}$  diluent c. Both of the dilutions were mixed and incubated for 4 min at room temperature. Next, 500  $\mu\text{L}$  BSA was used to block the staining process. The labeled exosomes were extracted again using the ExoQuick Exosome precipitation reagent and washed three times with PBS. Finally, the labeled exosomes were resuspended in 50  $\mu\text{L}$  PBS and then added to the prepared cells in each well of the 6-well plates for co-culturing at 37°C. To observe the fluorescence after 24 h of co-culturing, the cells were washed three times and then subjected to nucleus staining with Benzimide H33342 (Sigma-Aldrich).

#### NF- $\kappa$ B Inhibitor and Aspirin Treatment

Caffeic acid phenethyl ester (Selleck Chemicals, TX, USA) was used as a specific inhibitor of NF- $\kappa$ B. Aspirin was purchased from Meilune, China. DMSO was used to dissolve the drugs. With reference to our previous experiments<sup>13</sup> and other reports,<sup>49,50</sup> we used 4  $\mu\text{M}$  NF- $\kappa$ B inhibitor and 5–10 mM aspirin as the working concentrations in the cell treatments. EBV-positive cells were cultured in medium containing 4  $\mu\text{M}$  NF- $\kappa$ B inhibitor or 5 mM aspirin. At 24 or 36 h post-treatment, the cellular proteins and total RNA were extracted, respectively, and subjected to the relevant detection methods.

#### Western Blotting Analysis

Western blotting (WB) was performed according to a standardized procedure as previously described.<sup>45</sup> Exosomes or cells were lysed in lysis buffer containing the PMSF protease inhibitor. The proteins were resolved by SDS-PAGE using a 10% gel, and the bands were detected using a chemiluminescence immunoassay (CLIA). The immunoblots were probed with specific antibodies. The  $\beta$ -actin or GAPDH antibodies (Proteintech, Chicago, IL, USA) were used for the loading controls. The specific antibodies used were as follows: EBV-LMP1 monoclonal antibody (mAb) (Dako Lifetech, Glostrup, Denmark), anti-CD63 (OriGene, MD, USA), anti-Hsp70 and anti-Tsg101 (Cell Signaling Technology, Chicago, IL, USA), p-NF- $\kappa$ B (p65) (Cell Signaling Technology), NF- $\kappa$ B (rabbit mAb, Millipore, MA, USA), RUNX2 rabbit mAb (Abcam, Cambridge, UK), E-cadherin (Cell Signaling Technology), vimentin (Cell Signaling Technology), and N-cadherin (Cell Signaling Technology).

#### Quantitative Real-Time PCR

To detect the miR-203 abundance and the mRNA expression levels of genes, qPCR was employed as previously described.<sup>10,13</sup> Briefly, following RNA extraction, 1  $\mu\text{g}$  of each RNA sample was reverse transcribed into cDNA using Easy TransScript One-Step gDNA Removal and cDNA Synthesis SuperMix (Thermo Scientific), with oligo-dT primers according to the manufacturer's protocols. Quantitative real-time PCR was performed using TransStart Tip Green qPCR SuperMix (Thermo Scientific) on a Bio-Rad system. The primer sequences are shown in Table S1. A two-step cycling program was performed as follows: an initial denaturation at 95°C for 10 min,

then 40 cycles of 95°C for 15 s and 60°C for 60 s. Three parallel replicates were performed for each sample in each experiment, and the results are expressed as the mean of three independent experiments.  $\beta$ -actin and GAPDH were used as the internal protein controls, and U6 was used as a control for miR-203.

#### Immunofluorescence (IF) and Immunohistochemistry (IHC) Assays

The IF assay was performed as described previously.<sup>13</sup> Briefly, 24 h post-treatment with 5 mM aspirin, fresh cells grown on coverslips in a 6-well plate were washed gently three times in PBS and then fixed in 10% PBS-buffered formaldehyde for 15 min, permeabilized with 0.5% Triton X-100 for 5 min, and then blocked with fresh 10% goat serum. The cell specimens were incubated with the primary antibody or with PBS as a control overnight at 4°C. Subsequently, the slides were washed with PBS and incubated with FITC-conjugated secondary antibodies (Abcam) for 1 h at room temperature. After the nuclear staining with Benzimide H33342, the fluorescence was observed under a microscope. The IHC assay was used for CDH6 detection in serial paraffin sections from metastatic lung tumors. Anti-CDH6 antibody was used as the primary antibody and PBS was used as a control. A biotinylated anti-rabbit immunoglobulin G (IgG) conjugated to streptavidin-horseradish peroxidase (HRP) was used as the secondary antibody. Colorimetric development was followed using diaminobezidine (DAB).<sup>10</sup>

#### Collection of Clinical Plasma Samples and Ethics Statement

The samples from the NPC patients and normal subjects were obtained from the Second Xiangya Hospital of Central South University and the First People's Hospital of Chenzhou, Hunan. The plasma was isolated from venous blood samples by centrifugation at 1,000  $\times g$  at room temperature (RT) and stored at  $-80^{\circ}\text{C}$ . We state that the study subjects were anonymized and that each patient's participation was voluntary, with written informed consent obtained at the hospital. The research was approved by the Ethics Committees of Central South University, Hunan, China, and the First People's Hospital of Chenzhou, Hunan, China.

#### Animal Experiments and Ethics Statement

The 4-week-old female BALB/c nude mice (SLAC Laboratory Animal, Shanghai, China) were used for the *in vivo* animal experiments. The animals were divided randomly into two groups with 5 mice each. With reference to other reports,<sup>47,48</sup> our experimental procedure was performed as follows: one group received oral aspirin suspended in 200  $\mu\text{L}$  ethyl alcohol at 100 mg/kg/day; the control group received the same amount of ethyl alcohol. After 1 week,  $1 \times 10^7$  5-8F cells in 200  $\mu\text{L}$  RPMI1640 medium were injected into each mouse through the tail vein. The drug was continuously used until the end of the experiment. At 50 days post-treatment, the body weight of each mouse was measured and the mice were sacrificed. The lungs were fixed, sliced, and stained with H&E.<sup>40</sup> For all of the experiments, the animal handling and experimental procedures were approved by the Animal Experimental Ethics Committee of Central South University, Hunan, China.



### Statistical Analysis

The statistical analyses were performed using GraphPad Prism 5. Differences between groups were analyzed using Student's *t* test or one-way ANOVA. The data are expressed as the means  $\pm$  SD. Differences between tissue groups were analyzed using the Mann-Whitney *U* test. The *p* values < 0.05, 0.01, and 0.001 were considered to indicate different degrees of statistical significance.

### SUPPLEMENTAL INFORMATION

Supplemental Information can be found online at <https://doi.org/10.1016/j.omtn.2019.05.023>.

### AUTHOR CONTRIBUTIONS

L.Z., Y.X., and S.Z. performed the experiments, analyzed data, and wrote the manuscript. J.L. supervised the animal study. J.T. and L.L. collected the clinical samples and assisted with the animal studies. S.X. and Q.Y. performed the pathology analysis. J.L. and F.Z. edited the manuscript. J.L. supervised the study.

### CONFLICTS OF INTEREST

The authors declare no competing interests.

### ACKNOWLEDGMENTS

This work was supported by the National Key Research and Development Program and the National Natural Science Foundations of China (2017YFC1200204, 31670171, and 81728011). We thank Dr. Wolfgang Hammerschmidt (GSF-National Research Center for Environment and Health, Germany) for kindly providing the p2089 plasmid, which was used for the establishment of the C2089 cell lines.

### REFERENCES

- Young, L.S., and Rickinson, A.B. (2004). Epstein-Barr virus: 40 years on. *Nat. Rev. Cancer* 4, 757–768.
- Zuo, L., Yue, W., Du, S., Xin, S., Zhang, J., Liu, L., Li, G., and Lu, J. (2017). An update: Epstein-Barr virus and immune evasion via microRNA regulation. *Virol. Sin.* 32, 175–187.
- Nakanishi, Y., Wakisaka, N., Kondo, S., Endo, K., Sugimoto, H., Hatano, M., Ueno, T., Ishikawa, K., and Yoshizaki, T. (2017). Progression of understanding for the role of Epstein-Barr virus and management of nasopharyngeal carcinoma. *Cancer Metastasis Rev.* 36, 435–447.
- Zheng, Y., Qin, Z., Ye, Q., Chen, P., Wang, Z., Yan, Q., Luo, Z., Liu, X., Zhou, Y., Xiong, W., et al. (2014). Lactoferrin suppresses the Epstein-Barr virus-induced inflammatory response by interfering with pattern recognition of TLR2 and TLR9. *Lab. Invest.* 94, 1188–1199.
- Chua, M.L.K., Wee, J.T.S., Hui, E.P., and Chan, A.T.C. (2016). Nasopharyngeal carcinoma. *Lancet* 387, 1012–1024.
- Zheng, Y., Zhang, W., Ye, Q., Zhou, Y., Xiong, W., He, W., Deng, M., Zhou, M., Guo, X., Chen, P., et al. (2012). Inhibition of Epstein-Barr virus infection by lactoferrin. *J. Innate Immun.* 4, 387–398.
- Zheng, X., Wang, J., Wei, L., Peng, Q., Gao, Y., Fu, Y., Lu, Y., Qin, Z., Zhang, X., Lu, J., et al. (2018). Epstein-Barr virus microRNA miR-BART5-3p inhibits p53 expression. *J. Virol.* 92, e01022-18.
- Lu, Y., Qin, Z., Wang, J., Zheng, X., Lu, J., Zhang, X., Wei, L., Peng, Q., Zheng, Y., Ou, C., et al. (2017). Epstein-Barr virus miR-BART6-3p inhibits the RIG-I Pathway. *J. Innate Immun.* 9, 574–586.
- Wang, L.W., Jiang, S., and Gewurz, B.E. (2017). Epstein-Barr Virus LMP1-mediated oncogenicity. *J. Virol.* 91, e01718-16.
- Yu, H., Lu, J., Zuo, L., Yan, Q., Yu, Z., Li, X., Huang, J., Zhao, L., Tang, H., Luo, Z., et al. (2012). Epstein-Barr virus downregulates microRNA 203 through the oncoprotein latent membrane protein 1: a contribution to increased tumor incidence in epithelial cells. *J. Virol.* 86, 3088–3099.
- Kojima, M., Morisaki, T., Sasaki, N., Nakano, K., Mibu, R., Tanaka, M., and Katano, M. (2004). Increased nuclear factor- $\kappa$ B activation in human colorectal carcinoma and its correlation with tumor progression. *Anticancer Res.* 24 (2B), 675–681.
- Shair, K.H.Y., Bendt, K.M., Edwards, R.H., Bedford, E.C., Nielsen, J.N., and Raab-Traub, N. (2007). EBV latent membrane protein 1 activates Akt, NF $\kappa$ B, and Stat3 in B cell lymphomas. *PLoS Pathog.* 3, e166.
- Zuo, L.L., Zhang, J., Liu, L.Z., Zhou, Q., Du, S.J., Xin, S.Y., Ning, Z.P., Yang, J., Yu, H.B., Yue, W.X., et al. (2017). Cadherin 6 is activated by Epstein-Barr virus LMP1 to mediate EMT and metastasis as an interplay node of multiple pathways in nasopharyngeal carcinoma. *Oncogenesis* 6, 402.
- Taipaleenmäki, H., Browne, G., Akech, J., Zustin, J., van Wijnen, A.J., Stein, J.L., Hesse, E., Stein, G.S., and Lian, J.B. (2015). Targeting of Runx2 by miR-135 and miR-203 impairs progression of breast cancer and metastatic bone disease. *Cancer Res.* 75, 1433–1444.
- Qu, J.Q., Yi, H.M., Ye, X., Zhu, J.F., Yi, H., Li, L.N., Xiao, T., Yuan, L., Li, J.Y., Wang, Y.Y., et al. (2015). MiRNA-203 reduces nasopharyngeal carcinoma radioresistance by targeting il8/akt signaling. *Mol. Cancer Ther.* 14, 2653–2664.
- Jiang, Q., Zhou, Y., Yang, H., Li, L., Deng, X., Cheng, C., Xie, Y., Luo, X., Fang, W., and Liu, Z. (2016). A directly negative interaction of miR-203 and ZEB2 modulates tumor stemness and chemotherapy resistance in nasopharyngeal carcinoma. *Oncotarget* 7, 67288–67301.
- Liu, L., Zhou, Q., Xie, Y., Zuo, L., Zhu, F., and Lu, J. (2017). Extracellular vesicles: novel vehicles in herpesvirus infection. *Virol. Sin.* 32, 349–356.
- He, C., Zheng, S., Luo, Y., and Wang, B. (2018). Exosome theranostics: biology and translational medicine. *Theranostics* 8, 237–255.
- Xie, M., Ma, L., Xu, T., Pan, Y., Wang, Q., Wei, Y., and Shu, Y. (2018). Potential Regulatory Roles of MicroRNAs and Long Noncoding RNAs in Anticancer Therapies. *Mol. Ther. Nucleic Acids* 13, 233–243.
- Shao, N., Xue, L., Wang, R., Luo, K., Zhi, F., and Lan, Q. (2019). miR-454-3p is an exosomal biomarker and functions as a tumor suppressor in glioma. *Mol. Cancer Ther.* 18, 459–469.
- Wang, L., Wang, C., Jia, X., and Yu, J. (2018). Circulating exosomal miR-17 inhibits the induction of regulatory T cells via suppressing TGFBR II expression in Rheumatoid Arthritis. *Cell. Physiol. Biochem.* 50, 1754–1763.
- Rodrigues, M., Fan, J., Lyon, C., Wan, M., and Hu, Y. (2018). Role of extracellular vesicles in viral and bacterial infections: pathogenesis, diagnostics, and therapeutics. *Theranostics* 8, 2709–2721.
- Meckes, D.G., Jr., Shair, K.H., Marquitz, A.R., Kung, C.P., Edwards, R.H., and Raab-Traub, N. (2010). Human tumor virus utilizes exosomes for intercellular communication. *Proc. Natl. Acad. Sci. USA* 107, 20370–20375.
- Chen, G., Huang, A.C., Zhang, W., Zhang, G., Wu, M., Xu, W., Yu, Z., Yang, J., Wang, B., Sun, H., et al. (2018). Exosomal PD-L1 contributes to immunosuppression and is associated with anti-PD-1 response. *Nature* 560, 382–386.
- Theodoraki, M.N., Yerneni, S.S., Hoffmann, T.K., Gooding, W.E., and Whiteside, T.L. (2018). Clinical significance of PD-L1<sup>+</sup> exosomes in plasma of head and neck cancer patients. *Clin. Cancer Res.* 24, 896–905.
- Kopp, E., and Ghosh, S. (1994). Inhibition of NF- $\kappa$ B by sodium salicylate and aspirin. *Science* 265, 956–959.
- Burn, J., and Sheth, H. (2016). The role of aspirin in preventing colorectal cancer. *Br. Med. Bull.* 119, 17–24.
- Sancisi, V., Gandolfi, G., Ragazzi, M., Nicoli, D., Tamagnini, I., Piana, S., and Ciarrocchi, A. (2013). Cadherin 6 is a new RUNX2 target in TGF- $\beta$  signalling pathway. *PLoS ONE* 8, e75489.
- Saini, S., Majid, S., Yamamura, S., Tabatabai, L., Suh, S.O., Shahryari, V., Chen, Y., Deng, G., Tanaka, Y., and Dahiya, R. (2011). Regulatory role of mir-203 in prostate cancer progression and metastasis. *Clin. Cancer Res.* 17, 5287–5298.
- Yoshizaki, T. (2002). Promotion of metastasis in nasopharyngeal carcinoma by Epstein-Barr virus latent membrane protein-1. *Histol. Histopathol.* 17, 845–850.

31. Bi, X.W., Wang, H., Zhang, W.W., Wang, J.H., Liu, W.J., Xia, Z.J., Huang, H.Q., Jiang, W.Q., Zhang, Y.J., and Wang, L. (2016). PD-L1 is upregulated by EBV-driven LMP1 through NF- $\kappa$ B pathway and correlates with poor prognosis in natural killer/T-cell lymphoma. *J. Hematol. Oncol.* 9, 109.
32. Fang, W., Zhang, J., Hong, S., Zhan, J., Chen, N., Qin, T., Tang, Y., Zhang, Y., Kang, S., Zhou, T., et al. (2014). EBV-driven LMP1 and IFN- $\gamma$  up-regulate PD-L1 in nasopharyngeal carcinoma: Implications for oncotargeted therapy. *Oncotarget* 5, 12189–12202.
33. Simons, M., and Raposo, G. (2009). Exosomes—vesicular carriers for intercellular communication. *Curr. Opin. Cell Biol.* 21, 575–581.
34. Azmi, A.S., Bao, B., and Sarkar, F.H. (2013). Exosomes in cancer development, metastasis, and drug resistance: a comprehensive review. *Cancer Metastasis Rev.* 32, 623–642.
35. Liu, N., Chen, N.Y., Cui, R.X., Li, W.F., Li, Y., Wei, R.R., Zhang, M.Y., Sun, Y., Huang, B.J., Chen, M., et al. (2012). Prognostic value of a microRNA signature in nasopharyngeal carcinoma: a microRNA expression analysis. *Lancet Oncol* 13, 633–641.
36. Frappier, L. (2012). EBNA1 and host factors in Epstein-Barr virus latent DNA replication. *Curr. Opin. Virol.* 2, 733–739.
37. Tu, C., Zeng, Z., Qi, P., Li, X., Yu, Z., Guo, C., Xiong, F., Xiang, B., Zhou, M., Gong, Z., et al. (2017). Genome-Wide Analysis of 18 Epstein-Barr Viruses Isolated from Primary Nasopharyngeal Carcinoma Biopsy Specimens. *J. Virol.* 91, e00301–e00317.
38. Hurwitz, S.N., Cheerathodi, M.R., Nkosi, D., York, S.B., and Meckes, D.G., Jr. (2018). Tetraspanin CD63 bridges autophagic and endosomal processes to regulate exosomal secretion and intracellular signaling of Epstein-Barr virus LMP1. *J. Virol.* 92, e01969-17.
39. Hurwitz, S.N., Nkosi, D., Conlon, M.M., York, S.B., Liu, X., Tremblay, D.C., and Meckes, D.G., Jr. (2017). CD63 regulates Epstein-Barr virus LMP1 exosomal packaging, enhancement of vesicle production, and non-canonical NF- $\kappa$ B signaling. *J. Virol.* 91, e02251-16.
40. Huang, D.P., Ho, J.H., Poon, Y.F., Chew, E.C., Saw, D., Lui, M., Li, C.L., Mak, L.S., Lai, S.H., and Lau, W.H. (1980). Establishment of a cell line (NPC/HK1) from a differentiated squamous carcinoma of the nasopharynx. *Int. J. Cancer* 26, 127–132.
41. Zhong, Z., Zhang, F., and Yin, S.C. (2015). Effects of TESTIN gene expression on proliferation and migration of the 5-8F nasopharyngeal carcinoma cell line. *Asian Pac. J. Cancer Prev.* 16, 2555–2559.
42. Song, L.B., Yan, J., Jian, S.W., Zhang, L., Li, M.Z., Li, D., and Wang, H.M. (2002). [Molecular mechanisms of tumorigenesis and metastasis in nasopharyngeal carcinoma cell sublines]. *Chin. J. Cancer* 21, 158–162.
43. Cai, L., Ye, Y., Jiang, Q., Chen, Y., Lyu, X., Li, J., Wang, S., Liu, T., Cai, H., Yao, K., et al. (2015). Epstein-Barr virus-encoded microRNA BART1 induces tumour metastasis by regulating PTEN-dependent pathways in nasopharyngeal carcinoma. *Nat. Commun.* 6, 7353.
44. Cheung, S.T., Huang, D.P., Hui, A.B., Lo, K.W., Ko, C.W., Tsang, Y.S., Wong, N., Whitney, B.M., and Lee, J.C. (1999). Nasopharyngeal carcinoma cell line (C666-1) consistently harbouring Epstein-Barr virus. *Int. J. Cancer* 83, 121–126.
45. Delecluse, H.J., Hilsenrath, T., Pich, D., Zeidler, R., and Hammerschmidt, W. (1998). Propagation and recovery of intact, infectious Epstein-Barr virus from prokaryotic to human cells. *Proc. Natl. Acad. Sci. USA* 95, 8245–8250.
46. Zuo, L., Yu, H., Liu, L., Tang, Y., Wu, H., Yang, J., Zhu, M., Du, S., Zhao, L., Cao, L., et al. (2015). The copy number of Epstein-Barr virus latent genome correlates with the oncogenicity by the activation level of LMP1 and NF- $\kappa$ B. *Oncotarget* 6, 41033–41044.
47. Yu, Z., Lu, J., Yu, H., Yan, Q., Zuo, L., and Li, G. (2011). A precise excision of the complete Epstein-Barr virus genome in a plasmid based on a bacterial artificial chromosome. *J. Virol. Methods* 176, 103–107.
48. Lu, J.H., Tang, Y.L., Yu, H.B., Zhou, J.H., Fu, C.Y., Zeng, X., Yu, Z.Y., Yin, H.L., Wu, M.H., Zhang, J.Y., et al. (2010). Epstein-Barr virus facilitates the malignant potential of immortalized epithelial cells: from latent genome to viral production and maintenance. *Lab. Invest.* 90, 196–209.
49. Mattheolabakis, G., Papayannis, I., Yang, J., Vaeth, B.M., Wang, R., Bandovic, J., Ouyang, N., Rigas, B., and Mackenzie, G.G. (2016). Phospho-aspirin (MDC-22) prevents pancreatic carcinogenesis in mice. *Cancer Prev. Res. (Phila.)* 9, 624–634.
50. Cossentini, L.A., Da Silva, R.V., Yamada-Ogatta, S.F., Yamauchi, L.M., De Almeida Araújo, E.J., and Pinge-Filho, P. (2016). Aspirin treatment exacerbates oral infections by *Trypanosoma cruzi*. *Exp. Parasitol.* 164, 64–70.

OMTN, Volume 17

## **Supplemental Information**

**Targeting Exosomal EBV-LMP1 Transfer  
and miR-203 Expression via the NF- $\kappa$ B Pathway:**

**The Therapeutic Role of Aspirin in NPC**

**Lielian Zuo, Yan Xie, Jinyong Tang, Shuyu Xin, Lingzhi Liu, Siwei Zhang, Qijia Yan, Fanxiu Zhu, and Jianhong Lu**

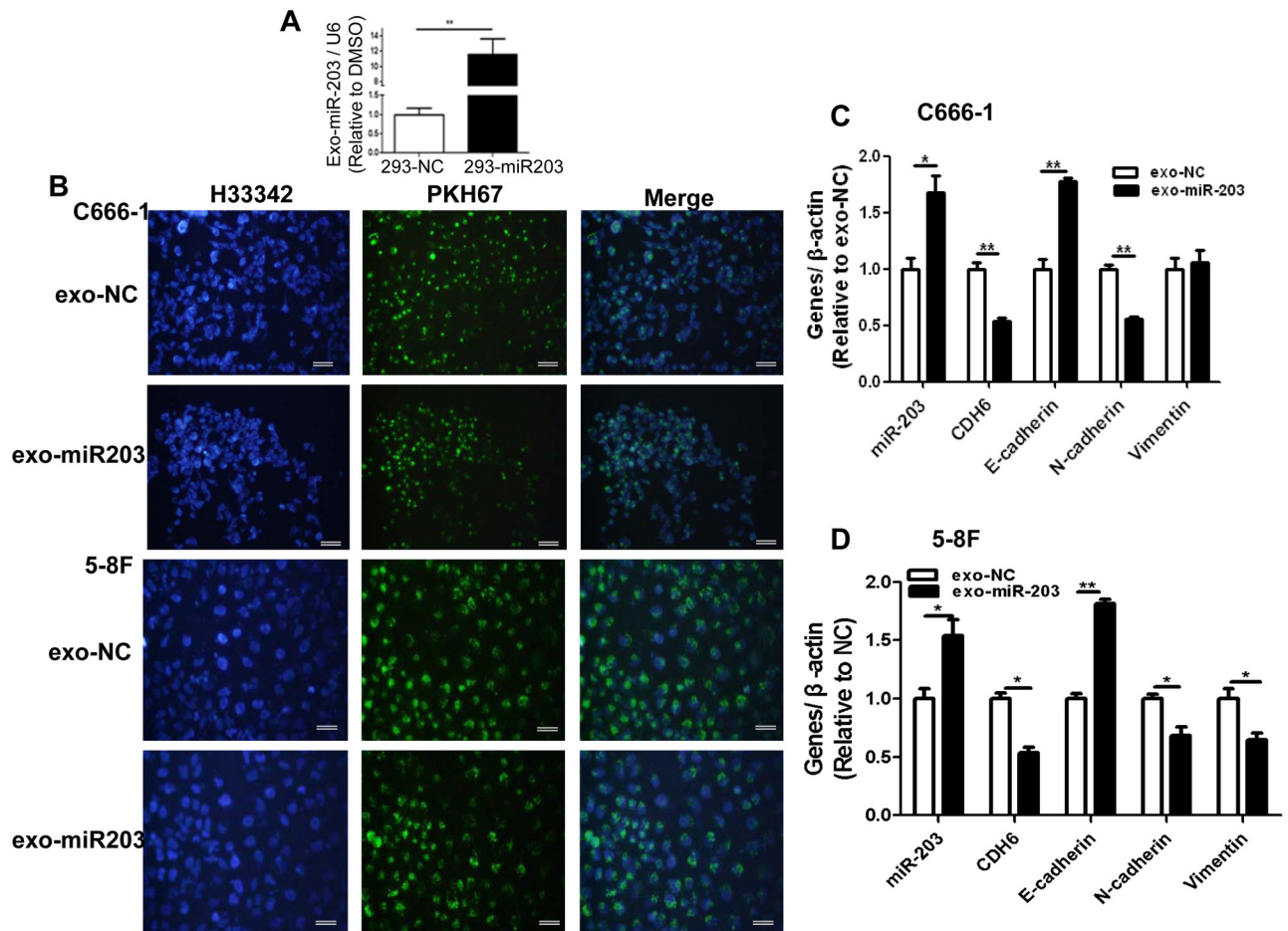


**Figure S1. Exosomal miR-203 uptake inhibits EMT potential in recipient NPC cells.** (A) The detection of exosome miR-203 by qPCR. The exosomes (Exo) were derived from 293-miR203 and 293-NC control cells respectively. (B) NPC C666-1 or 5-8F cells co-cultured with exo-miR203. Green indicates PKH67-labelled exosomes and blue indicates cell nuclei with H33342 staining. Scale bar, 50 $\mu$ m. (C) The detection of miR-203, CDH6, and the EMT markers in C666-1 cells by qPCR after co-culture. (D) The detection of miR-203, CDH6, and the EMT markers in 5-8F cells after co-culture. The results are the means  $\pm$  SD (n = 3). \*p < 0.05, \*\* p<0.01.



**Table S1.****Primers used for qPCR.**

<b>Gene names</b>	<b>Primer names</b>	<b>Primer sequences</b>
LMP1	LMP1-L	TGAACACCACCACGATGACT
	LMP1-R	GTGCGCCTAGGTTTTGAGAG
CDH6	CDH6-L	TTCCTCAGGGTGCCGATATC
	CDH6-R	GTTGCCATCCTTCTGTGCAT
E-cadherin	E-cadherin-L	TTCTGGAAGGAATGGAGGAGTC
	E-cadherin-R	ACCTGGAATTGGGCAAATGTG
N-cadherin	N-cadherin-L	GACAATGCCCTCAAGTGTT
	N-cadherin-R	CCATTAAGCCGAGTGATGGT
Vimentin	Vimentin-L	AGATGGCCCTTGACATTGAG
	Vimentin-R	TGGAAGAGGCAGAGAAATCC
$\beta$ -actin	$\beta$ -actin-L	TCACCAACTGGGACGACATG
	$\beta$ -actin-R	GTCACCGGAGTCCATCACGAT